

# Lattice Gas Cellular Automata for Computational Fluid Animation

Gilson A. Giraldi, Adilson V. Xavier, Antonio L. Apolinario Jr, Paulo S. Rodrigues  
 National Laboratory of Scientific Computing  
 Ave Getúlio Vargas, 333, 25651-075, Petrópolis, RJ, Brasil  
 {gilson,adilson,alopes,pssr}@lncc.br

## Abstract

*The past two decades showed a rapid growing of physically-based modeling of fluids for computer graphics applications. In this area, a common top down approach is to model the fluid dynamics by Navier-Stokes equations and apply a numerical techniques such as Finite Differences or Finite Elements for the simulation. In this paper we focus on fluid modeling through Lattice Gas Cellular Automata (LGCA) for computer graphics applications. LGCA are discrete models based on point particles that move on a lattice, according to suitable and simple rules in order to mimic a fully molecular dynamics. By Chapman-Enskog expansion, a known multiscale technique in this area, it can be demonstrated that the Navier-Stokes model can be reproduced by the LGCA technique. Thus, with LGCA we get a fluid model that does not require solution of complicated equations. Therefore, we combine the advantage of the low computational cost of LGCA and its ability to mimic the realistic fluid dynamics to develop a new animating framework for computer graphics applications. In this work, we discuss the theoretical elements of our proposal and show experimental results.*

## 1. Introduction

Physically-based techniques for the animation of natural elements like fluids (gas or liquids), elastic, plastic and melting objects, among others, have taken the attention of the computer graphics community [14]. The motivation for such interest rely in the potential applications of these methods and in the complexity and beauty of the natural phenomena that are involved [25, 3]. In particular, techniques in the field of Computational Fluid Dynamics (CFD) have been applied for fluid animation in applications such as virtual surgery simulators, computer games and visual effects [1, 17].

In this paper we focus on physically-based fluid animation for computer graphics applications (see [1] and ref-

erences therein). Basically, the works in this area fall in two categories: Realistic fluid and Interactive, or Real-Time, fluid animation. The former is more suitable for the special effects industry [17] while the later is appropriate for interactive applications like computer games and virtual surgery [23, 15]. The work [5] is a remarkable one in this area which includes fluid equations and numerical technique [9], shortly Computational Fluid Dynamics (CFD), and scientific visualization methods [20]. The literature of this field reports gas [5, 25] and water simulations [13], interaction between liquids and deformable solids [16], and others [24, 1].

A majority of fluid animation methods in computer graphics use 2D/3D mesh based approaches that are mathematically motivated by the Eulerian methods of Finite Element (FE) and Finite Difference (FD), in conjunction with Navier-Stokes equations of fluids [9]. These works are based on a top down viewpoint of the nature: the fluid is considered as a continuous system subjected to Newton's and conservation Laws as well as state equations connecting the macroscopic variables of pressure  $P$ , density  $\rho$  and temperature  $T$ .

In this paper, we change the viewpoint to the bottom up model of the Lattice Gas Cellular Automata (LGCA) [6]. These are discrete models based on point particles that move on a lattice, according to suitable and simple rules in order to mimic a fully molecular dynamics. Particles can only move along the edges of the lattice and their interactions are based on simple collision rules. There is an exclusion principle that limits to one the number of particles that enter a given site (lattice node) in a given direction of motion. Such framework needs low computational resources for both the memory allocation and the computation itself. Such models have been applied for scientific application in two-phase flows description (gas-liquid systems, for example), numerical simulation of bubble flows [10], among others. Besides, Wolfram [26] has studied the computational and thermodynamics aspects of these models for fluid modeling.

In this paper we focus on fluid modeling through Lat-

tice Gas Cellular Automata (LGCA) for computer graphics applications. Specifically we take a special LCGA, introduced by Frisch, Hasslacher and Pomeau, known as FHP model, and show its capabilities for computer graphics applications. By Chapman-Enskog expansion, a known multi-scale technique in this area, it can be demonstrated that the Navier-Stokes model can be reproduced by FHP technique. However, there is no need to solve Partial Differential Equations (PDEs) to obtain a high level of description. Therefore, we combine the advantage of the low computational cost of LGCA and its ability to mimic the realistic fluid dynamics to develop a new animating framework for computer graphics applications. Up to our knowledge, there are no references using FHP for fluid animation in Computer Graphics. In this work, we discuss the theoretical elements of our proposal and present some experimental results.

The paper is organized as follows. Section 2 offer a review of CFD for fluid animation. Section 3 describes the FHP model its multiscale analysis. The experimental results are presented on section 4. Conclusions are given on Section 5.

## 2. Navier-Stokes for Fluid Animation

The majority fluid models in computer graphics follow the Eulerian formulation of fluid mechanics; that is, the fluid is considered as a continuous system subjected to Newton's and conservation Laws as well as state equations connecting the macroscopic variables that define the thermodynamic state of the fluid: pressure  $P$ , density  $\rho$  and temperature  $T$ .

So, the mass conservation, also called continuity equation, is given by [9]:

$$\frac{\partial \rho}{\partial t} + \nabla \cdot (\rho \vec{u}) = 0 \quad (1)$$

The linear momentum conservation equation, also called Navier-Stokes, can be obtained by applying the third Newton's Law to a volume element  $dV$  of fluid. It can be written as [9]:

$$\rho \left( \frac{\partial \vec{u}}{\partial t} + \vec{u} \cdot \nabla \vec{u} \right) = -\nabla P + \mathbf{F} + \mu \left( \nabla^2 \vec{u} + \frac{1}{3} \nabla (\nabla \cdot \vec{u}) \right) \quad (2)$$

where  $\mathbf{F}$  is an external force field and  $\mu$  is the viscosity of the fluid. Besides, the equation  $\nabla \cdot \vec{u} = 0$  must be added to model incompressible fluids. Thus, if we combine this equations with expression (2) we obtain the Navier-Stokes equations for incompressible fluids (water, for example):

$$\rho \left( \frac{\partial \vec{u}}{\partial t} + \vec{u} \cdot \nabla \vec{u} \right) = -\nabla P + \mathbf{F} + \mu \nabla^2 \vec{u}, \quad (3)$$

$$\nabla \cdot \vec{u} = 0. \quad (4)$$

Also, we need an additional equation for the pressure field. This is a state equation which ties together all of the conservation equations for continuum fluid dynamics and must be chosen to model the appropriate fluid (*i.e.* compressible or incompressible). In the case of liquids, the pressure  $P$  is temperature insensitive and can be approximated by  $P = P(\rho)$ . Morris in [12] proposed an expression that have been used for fluid animation also [13]:

$$P = c^2 \rho \quad (5)$$

where  $c$  is the speed of sound in this fluid [21].

Equations (3)-(5) need initial conditions  $(\rho(t=0, x, y, z), \vec{u}(t=0, x, y, z))$ . Besides, in practice, fluid domain is a closed subset of the Euclidean space and thus the behavior of the fluid in the domain boundary - *boundary conditions* - must be explicitly given. For a fixed rigid surface  $S$ , one usual model is the no-sleep boundary condition that can be written as:

$$\vec{u}|_S = 0. \quad (6)$$

Also, numerical methods should be used to perform the computational simulation of the fluid because the fluid equations in general do not have analytical solution. Finite Element (FE) and Finite Difference (FD) are known approaches in this field. Recently, the Lagrangian *Method of Characteristics* [22, 23] and the meshfree methods of *Smoothed Particle Hydrodynamics (SPH)* [13] and *Moving-Particle Semi-Implicit (MPS)* [19] have been also applied.

If the fluid is temperature sensitive, then an energy conservation law should be applied. For example, in [5] authors develop a framework for hot turbulent gas animation. The model comprises equations (3),(4),(6) as well as the following equation for temperature change and the *buoyant* force, respectively:

$$\frac{\partial T}{\partial t} = \lambda \nabla^2 T - \nabla \cdot (T \vec{u}), \quad (7)$$

$$\mathbf{F} = -\beta g (T_0 - T), \quad (8)$$

where  $\lambda$  is the diffusion coefficient,  $T_0$  is a reference temperature and  $\beta$  is the coefficient of thermal expansion. The numerical method used in [5] is Finite Difference. This work can reproduce a hot gas behavior with some realism but has the limitation that the integration time step is constrained to:

$$\Delta t < \frac{h}{\|\vec{u}\|}, \quad (9)$$

where  $h$  is the mesh resolution. Besides, the restriction of equation (4) is not suitable for a compressible system like a gas.

Henceforth, after that work, we can find works that: (a) Propose more stable models to achieve faster simulations; (b) Use truly meshfree Lagrangian methods; (c) Include realistic behaviors of truly incompressible flow simulation and interaction of fluids with deformable solids; (d) Use GPU capabilities in order to achieve faster simulations for interactive applications; (e) Generate special effects through fluid flows; among others [1].

From the viewpoint of fluid models, all the cited works are top down approaches in the sense that the relationships of interest are between variables that capture the global properties of the system; that is, pressure, density and temperature. These relationships are expressed in ordinary or partial differential equations like (3).

On the other hand, bottom up models start from a description of local interactions. These models usually involve algorithmic descriptions of individuals, *particles* in the case of fluids. Analysis and computer simulation of bottom up models should produce, as emergent properties, the global relationships seen in the real world, without these being built into the model. Thus, there is no need to use a PDEs and numerical methods to obtain a high level of description.

For Computer Graphics applications, such approach is explored in [11] for real-time simulation and animation of phenomena involving convection, reaction-diffusion, and boiling. An extension of cellular automata known as the coupled map lattice (CML) is used for simulation. CML represents the state of a dynamic system as continuous values on a discrete lattice. In [11] the lattice values are stored in a texture, and pixel-level programming are used to implement simple next-state computations on lattice nodes and their neighbors. However, Navier-Stokes models are not considered and CML still uses continuous values for representations. That is also the case of Lattice Boltzmann models [8]. In this paper we propose the application of an even more simple model, the FHP one, for fluid simulation. It will be demonstrated how Navier-Stokes models can be reproduced by this method. FHP is described in the next section.

### 3. FHP and Navier-Stokes

The FHP was introduced by Frisch, Hasslacher and Pomeau [7] in 1986 and is a model of a two-dimensional fluid. It can be seen as an abstraction, at a microscopic scale, of a fluid. The FHP model describes the motion of particles traveling in a discrete space and colliding with each other. The space is discretized in a hexagonal lattice.

The microdynamics of FHP is given in terms of Boolean variables describing the occupation numbers at each site of the lattice and at each time step (i.e. the presence or the absence of a fluid particle). The FHP particles move in dis-

crete time steps, with a velocity of constant modulus, pointing along one of the six directions of the lattice. The dynamics is such that no more than one particle enters the same site at the same time with the same velocity. This restriction is the *exclusion principle*; it ensures that six Boolean variables at each lattice site are always enough to represent the microdynamics.

In the absence of collisions, the particles would move in straight lines, along the direction specified by their velocity vector. The velocity modulus is such that, in a time step, each particle travels one lattice spacing and reaches a nearest-neighbor site.

In order to conserve the number of particles and the momentum during each interaction, only a few configurations lead to a non-trivial collision (i.e. a collision in which the directions of motion have changed). When exactly two particles enter the same site with opposite velocities, both of them are deflected by 60 degrees so that the output of the collision is still a zero momentum configuration with two particles. When exactly three particles collide with an angle of 120 degrees between each other, they bounce back to where they come from (so that the momentum after the collision is zero, as it was before the collision). Both two- and three-body collisions are necessary to avoid extra conservation laws. Several variants of the FHP model exist in the literature [4], including some with rest particles like models FHP-II and FHP-III. For all other configurations no collision occurs and the particles go through as if they were transparent to each other.

The full microdynamics of the FHP model can be expressed by evolution equations for the occupation numbers defined as the number,  $n_i(\vec{r}, t)$ , of particle entering site  $\vec{r}$  at time  $t$  with a velocity pointing along direction  $\vec{c}_i$ , where  $i = 1, 2, \dots, 6$  labels the six lattice directions. The numbers  $n_i$  can be 0 or 1.

We also define the time step as  $\Delta_t$  and the lattice spacing as  $\Delta_r$ . Thus, the six possible velocities  $\vec{v}_i$  of the particles are related to their directions of motion by

$$\vec{v}_i = \frac{\Delta_r}{\Delta_t} \vec{c}_i. \quad (10)$$

Without interactions between particles, the evolution equations for the  $n_i$  would be given by

$$n_i(\vec{r} + \Delta_r \vec{c}_i, t + \Delta_t) = n_i(\vec{r}, t) \quad (11)$$

which express that a particle entering site  $\vec{r}$  with velocity along  $\vec{c}_i$  will continue in a straight line so that, at next time step, it will enter site  $\vec{r} + \Delta_r \vec{c}_i$  with the same direction of motion. However, due to collisions, a particle can be removed from its original direction or another one can be deflected into direction  $\vec{c}_i$ .

For instance, if only  $n_i$  and  $n_{i+3}$  are 1 at site  $\vec{r}$ , a collision occurs and the particle traveling with velocity  $\vec{v}_i$

will then move with either velocity  $\vec{v}_{i-1}$  or  $\vec{v}_{i+1}$ , where  $i = 1, 2, \dots, 6$ . The quantity

$$D_i = n_i n_{i+3} (1 - n_{i+1}) (1 - n_{i+2}) (1 - n_{i+4}) (1 - n_{i+5}). \quad (12)$$

indicates, when  $D_i = 1$  that such a collision will take place. Therefore  $n_i - D_i$  is the number of particles left in direction  $\vec{c}_i$  due to a two-particle collision along this direction.

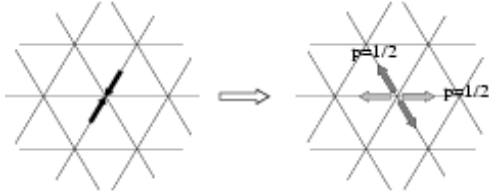


Figura 1: The two-body collision in the FHP.

Now, when  $n_i = 0$ , a new particle can appear in direction  $\vec{c}_i$ , as the result of a collision between  $n_{i+1}$  and  $n_{i+4}$  or a collision between  $n_{i-1}$  e  $n_{i+2}$ . It is convenient to introduce a random Boolean variable  $q(\vec{r}, t)$ , which decides whether the particles are deflected to the right ( $q = 1$ ) or to the left ( $q = 0$ ), when a two-body collision takes place. Therefore, the number of particle created in direction  $\vec{c}_i$  is

$$q D_{i-1} + (1 - q) D_{i+1}. \quad (13)$$

Particles can also be deflected into (or removed from) direction  $\vec{c}_i$  because of a three-body collision. The quantity which express the occurrence of a three-body collision with particles  $n_i$ ,  $n_{i+2}$  and  $n_{i+4}$  is

$$T_i = n_i n_{i+2} n_{i+4} (1 - n_{i+1}) (1 - n_{i+3}) (1 - n_{i+5}) \quad (14)$$

As before, the result of a three-body collision is to modify the number of particles in direction  $\vec{c}_i$  as

$$n_i - T_i + T_{i+3}, \quad (15)$$

Thus, according to our collision rules, the microdynamics of a LGCA is written as

$$n_i(\vec{r} + \Delta_r \vec{c}_i, t + \Delta_t) = n_i(\vec{r}, t) + \Omega_i(n(\vec{r}, t)) \quad (16)$$

where  $\Omega_i$  is called the collision term.

For the FHP model,  $\Omega_i$  is defined so as to reproduce the collisions, that is

$$\Omega_i = -D_i + q D_{i-1} + (1 - q) D_{i+1} - T_i + T_{i+3}. \quad (17)$$

Using the full expression for  $D_i$  and  $T_i$ , given by the Equations (12)-(14), we obtain,

$$\begin{aligned} \Omega_i &= -n_i n_{i+2} n_{i+4} (1 - n_{i+1}) (1 - n_{i+3}) (1 - n_{i+5}) \\ &+ n_{i+1} n_{i+3} n_{i+5} (1 - n_i) (1 - n_{i+2}) (1 - n_{i+4}) \\ &- n_i n_{i+3} (1 - n_{i+1}) (1 - n_{i+2}) (1 - n_{i+4}) (1 - n_{i+5}) \\ &+ (1 - q) n_{i+1} n_{i+4} (1 - n_i) (1 - n_{i+2}) (1 - n_{i+3}) \\ &+ (1 - q) (1 - n_{i+5}) \\ &+ q n_{i+2} n_{i+5} (1 - n_i) (1 - n_{i+1}) (1 - n_{i+3}) (1 - n_{i+4}). \end{aligned} \quad (18)$$

These equations are easy to code in a computer and yield a fast and exact implementation of the model

Until now, we deal with microscopic quantities. However, the physical quantities of interest are not so much the Boolean variables  $n_i$  but macroscopic quantities or average values, such as, for instance, the average density of particles and the average velocity field at each point of the system. These quantities are defined from the ensemble average  $N_i(\vec{r}, t) = \langle n_i(\vec{r}, t) \rangle$  of the microscopic occupation variables. Note that,  $N_i(\vec{r}, t)$  is also the probability of having a particle entering the site  $\vec{r}$ , at time  $t$ , with velocity

$$\vec{v}_i = \frac{\Delta_r}{\Delta_t} \vec{c}_i.$$

In general, a LGCA is characterized by the number  $z$  of lattice directions and the spatial dimensionality  $d$ . In our case  $d = 2$  and  $z = 6$ . Following the usual definition of statistical mechanics, the local density of particles is the sum of the average number of particles traveling along, each direction  $\vec{c}_i$

$$\rho(\vec{r}, t) = \sum_{i=0}^z N_i(\vec{r}, t). \quad (19)$$

Similarly, the particle current, which is the density  $\rho$  times the velocity field  $\vec{u}$ , is expressed by.

$$\rho(\vec{r}, t) \vec{u}(\vec{r}, t) = \sum_{i=0}^z \vec{v}_i N_i(\vec{r}, t). \quad (20)$$

Another quantity which will play an importante role in the up coming derivation is the momentum tensor  $\Pi$  defined as

$$\Pi_{\alpha\beta} = \sum_{i=0}^z \vec{v}_{i\alpha} \vec{v}_{i\beta} N_i(\vec{r}, t) \quad (21)$$

where the greek indices  $\alpha$  and  $\beta$  label the  $d$  spatial components of the vectors. The quantity  $\Pi$  represents the flux of the  $\alpha$ -component of momentum transported along the  $\beta$ -axis. This term will contain the pressure contribution and the effects of viscosity.

The starting point to obtain the macroscopic behavior of the CA fluid is to derive an equation for the  $N'_i$ 's. Averaging the microdynamics (16) yields

$$N_i(\vec{r} + \Delta_r \vec{c}_i, t + \Delta_t) - N_i(\vec{r}, t) = \langle \Omega_i(n(\vec{r}, t)) \rangle \quad (22)$$

where  $\Omega_i$  is the collision term of the LGCA, under study. It is important to notice that  $\Omega_i(n)$  has some generic properties, namely

$$\sum_{i=1}^z \Omega_i = 0 \quad \text{and} \quad \sum_{i=1}^z \vec{v}_i \Omega_i = 0 \quad (23)$$

expressing the fact that particle number and momentum are conserved during the collision process (the incoming sum of mass or momentum equals the outgoing sum).

The  $N_i$ 's vary between 0 and 1 and, at a scale  $L \gg \Delta_r$  and  $T \gg \Delta_t$ , one can expect them to be smooth functions of the space and time coordinates. Therefore, equation (22) can be Taylor expanded up to second order and gives

$$\begin{aligned} & \Delta_r (\vec{c}_i \cdot \nabla) N_i(\vec{r}, t) + \Delta_t \partial_t N_i(\vec{r}, t) \\ & + \frac{1}{2} (\Delta_r)^2 (\vec{c}_i \cdot \nabla)^2 N_i(\vec{r}, t) + \Delta_r \Delta_t (\vec{c}_i \cdot \nabla) \partial_t N_i(\vec{r}, t) \\ & + \frac{1}{2} (\Delta_t)^2 (\partial_t)^2 N_i(\vec{r}, t) = \langle \Omega_i(n(\vec{r}, t)) \rangle. \end{aligned} \quad (24)$$

where  $(\partial_t)^2$  is the second derivative in respect to the time parameter  $t$ .

At a macroscopic scale  $L \gg \Delta_r$ , following the procedure of the so-called multiscale expansion [18], we introduce a new space variable  $\vec{r}_1$  such that

$$\vec{r}_1 = \epsilon \partial_{\vec{r}_1} \quad \text{and} \quad \partial_r = \epsilon \partial_{\vec{r}_1} \quad (25)$$

with  $\epsilon \ll 1$ . We also introduce the extra time variables  $t_1 = \epsilon t$  and  $t_2 = \epsilon^2 t$ , as well as new functions  $N_i^\epsilon$  depending on  $\vec{r}_1, t_1$  and  $t_2$ ,  $N_i^\epsilon = N_i^\epsilon(t_1, t_2, \vec{r}_1)$  and substitute into equation (24)

$$N_i \rightarrow N_i^\epsilon \quad \partial_t \rightarrow \epsilon \partial_{t_1} + \epsilon^2 \partial_{t_2} \quad \partial_r \rightarrow \epsilon \partial_{\vec{r}_1} \quad (26)$$

together with the corresponding expressions for the second order derivatives. Then obtain new equations for the new functions  $N_i^\epsilon$ . Thus, we may write [18],

$$N_i^\epsilon = N_i^{(0)} + \epsilon N_i^{(1)} + \epsilon^2 N_i^{(2)} + \dots \quad (27)$$

The Chapman-Enskog method is the standard procedure used in statistical mechanics to solve an equation like (24) with a perturbation parameter  $\epsilon$ . Assuming that  $\langle \Omega_i(n) \rangle$  can be factorized into  $\Omega_i(N)$ , we write the contributions of each order in  $\epsilon$ . According to multiscale expansion (??, the right-hand side of (24) reads

$$\Omega_i(N) = \Omega_i(N^{(0)}) + \epsilon \sum_{j=1}^z \left( \frac{\partial \Omega_i(N^{(0)})}{\partial N_j} \right) N_j^{(1)} + \mathcal{O}(\epsilon^2) \quad (28)$$

Using expressions (25)-(27) in the left-hand side of (24) and comparing the terms of the same order in  $\epsilon$  in the equation (28), yields

$$\mathcal{O}(\epsilon^0) : \Omega_i(N^{(0)}) = 0 \quad (29)$$

and

$$\begin{aligned} \mathcal{O}(\epsilon^1) : & \partial_{1\alpha} v_{i\alpha} N_i^{(0)} + \partial_{t_1} N_i^{(0)} \\ & = \frac{1}{\Delta_t} \sum_{j=1}^z \left( \frac{\partial \Omega_i(N^{(0)})}{\partial N_j} \right) N_j^{(1)} \end{aligned} \quad (30)$$

where the subscript 1 in spatial derivatives (e.g.  $\partial_{1\alpha}$ ) indicates a differential operator expressed in the variable  $\vec{r}_1$  and  $\frac{\Delta_r}{\Delta_t} (\vec{c}_i \cdot \nabla_{r_1}) = \partial_{1\alpha} v_{i\alpha}$ , from equation (10).

We also impose the extra conditions that the macroscopic quantities  $\rho$  and  $\rho \vec{u}$  are entirely given by the zero order of expansion (27)

$$\rho = \sum_{i=1}^z N_i^{(0)} \quad \text{and} \quad \rho \vec{u} = \sum_{i=1}^z \vec{v}_i N_i^{(0)} \quad (31)$$

and therefore

$$\sum_{i=1}^z N_i^{(l)} = 0 \quad \text{and} \quad \sum_{i=1}^z \vec{v}_i N_i^{(l)} = 0, \quad \text{for } l \geq 1 \quad (32)$$

Thus, following the Chapman-Enskog method we can obtain [6], from equation (24), the following result at order  $\epsilon$

$$\partial_{t_1} \rho + \text{div}_1 \rho \vec{u} = 0 \quad (33)$$

and

$$\partial_{t_1} \rho \vec{u}_\alpha + \partial_{1\beta} \Pi_{\alpha\beta}^{(0)} = 0 \quad (34)$$

On the other hand, if we consider the terms of order  $\epsilon^2$  and using the relations (33) and (34) to simplify, we have

$$\partial_{t_2} \rho \vec{u}_a + \partial_{1\beta} \left[ \Pi_{\alpha\beta}^{(1)} + \frac{\Delta_t}{2} \left( \partial_{t_1} \Pi_{\alpha\beta}^{(0)} + \partial_{1\gamma} S_{\alpha\beta\gamma}^{(0)} \right) \right] = 0 \quad (35)$$

The last equation contains the dissipative contributions to the Euler equation (34). The first contribution is  $\Pi_{\alpha\beta}^{(1)}$  which is the dissipative part of the momentum tensor. The second part, namely  $\frac{\Delta_t}{2} \left( \partial_{t_1} \Pi_{\alpha\beta}^{(0)} + \partial_{1\gamma} S_{\alpha\beta\gamma}^{(0)} \right)$  comes from the second order terms of the Taylor expansion of the discrete Boltzmann equation. These terms account for the discreteness of the lattice and have no counterpart in standard hydrodynamics. As we shall see, they will lead to the so-called lattice viscosity. The order  $\epsilon$   $\epsilon^2$  can be grouped together to give the general equations governing our system. Summing equations (33) and (35) with the appropriate power of  $\epsilon$  as factor and we obtain the continuity equation (see expression (1)):

$$\partial_t \rho + \text{div} \rho \vec{u} = 0 \quad (36)$$

Similarly, equation (34) and (35) yields [6]

$$\partial_t \rho u_a + \frac{\partial}{\partial r_\beta} \left[ \Pi_{\alpha\beta} + \frac{\Delta_t}{2} \left( \epsilon \partial_{t_1} \Pi_{\alpha\beta}^{(0)} + \frac{\partial}{\partial r_\gamma} S_{\alpha\beta\gamma}^{(0)} \right) \right] = 0 \quad (37)$$

We now turn to the problem of solving equation (29) together with conditions (31) in order to find  $N_i^{(0)}$  as functions of  $\rho$  and  $\rho \vec{u}$ . The solutions  $N_i^{(0)}$  which make the collision term  $\Omega$  vanish are known as the local equilibrium solutions. Physically, they correspond to a situation where the rate of each type of collision equilibrates. Since the collision time  $\Delta_t$  is much smaller than the macroscopic observation time, it is reasonable to expect, in first approximation that an equilibrium is reached locally.

Provided that the collision behaves reasonably, it is found [6] that the generic solution is

$$N_i^{(0)} = \frac{1}{1 + \exp(-A - \vec{B} \cdot \vec{v}_i)} \quad (38)$$

This expression has the form of a Fermi-Dirac distribution. This is a consequence of the exclusion principle we have imposed in the cellular automata rule (no more than one particle per site and direction). This form is explicitly obtained for the FHP model by assuming that the rate of direct and inverse collisions are equal. The quantities  $A$  e  $\vec{B}$  are functions of the density  $\rho$  and the velocity field  $\vec{u}$  and are to be determined according to equations (31). In order to carry out this calculation,  $N_i^{(0)}$  is Taylor expanded up to second order in the velocity field  $\vec{u}$ . One obtains [2]

$$N_i^{(0)} = a\rho + \frac{b\rho}{v^2} \vec{v}_i \cdot \vec{u} + \frac{\rho G(\rho)}{v^4} Q_{i\alpha\beta} u_\alpha u_\beta \quad (39)$$

where  $\alpha, \beta, \gamma$  are summed over the spacial coordinates, e.g.  $\alpha, \beta, \gamma \in \{1, \dots, d\}$ ,  $v = \frac{\Delta r}{\Delta t}$ ,  $a = \frac{1}{z}$ ,  $b = \frac{d}{z}$  and

$$Q_{i\alpha\beta} = v_{i\alpha} v_{i\beta} - \frac{v^2}{d} \delta_{\alpha\beta} \quad (40)$$

The function  $G$  is obtained from the fact that  $N_i^{(0)}$  is the Taylor expansion of a Fermi-Dirac distribution. For FHP, it is found [2, 6]

$$G(\rho) = \frac{2(3-\rho)}{3(6-\rho)}$$

We may now compute the local equilibrium part of the momentum tensor,  $\Pi_{\alpha\beta}^{(0)}$  and then obtain the pressure term

$$p = aC_2 v^2 \rho - \left[ \frac{C_2}{d} - C_4 \right] \rho G(\rho) u^2 \quad (41)$$

where  $C_2 = \frac{z}{d}$ .

We can see [6] that the lattice viscosity is given by

$$\begin{aligned} \nu_{lattice} &= -C_4 b \frac{\Delta_t v^2}{2} = -\frac{z}{d(d+2)} \frac{d}{z} \frac{\Delta_t}{2} v^2 \\ &= \frac{-\Delta_t}{2(d+2)} v^2 \end{aligned}$$

The usual contribution to viscosity is due to the collision between the fluid particles is given by [6]

$$\nu_{coll} = \Delta_t v^2 \frac{bC_4}{\Lambda}$$

where  $-\Lambda$  is given by  $-\Lambda = 2s(1-s)^3$  where  $s = \frac{\rho}{6}$

Therefore, the Navier-Stokes equation reads

$$\partial_t \vec{u} + 2C_4 G(\rho) (\vec{u} \cdot \nabla) \vec{u} = -\frac{1}{\rho} \nabla p + \nu \nabla^2 \vec{u} \quad (42)$$

where

$$\nu = \Delta_t v^2 b C_4 \left( \frac{1}{\Lambda} - \frac{1}{2} \right) = \frac{\Delta_t v^2}{d+2} \left( \frac{1}{\Lambda} - \frac{1}{2} \right) \quad (43)$$

is the kinematic viscosity of our discrete fluid.

## 4. Experimental Results

In this section we describe some experiments with FHP for bidimensional fluid simulation. Firstly, we highlight the simplicity of creating new configurations. Figure 2 shows an initial configuration with zero density in the middle of the system. It is not required any extra mathematical machinery to deal with such density discontinuity because system rules do not undergo modifications. Figures 1 were generated with 80.000 particles with position and velocity directions randomly distributed. The lattice resolution is 100 by 100 points.

The density distribution at time 10 and 25 (Figures 3 and 4) show an interesting pattern near the front of the discontinuity. The evolution for time 50 is even more interesting (Figure 5). If we want to predict such effects, we need to consider Navier-Stokes equations. However, if the aim is to explore the visual effect, we can just simulate and take the desired result at its time. As expected, the system evolves towards a configuration in thermodynamic equilibrium (or maximum entropy [26]). Figure 6 shows such state. From the macroscopic viewpoint, the fluid achieves a static configuration in which the macroscopic velocity  $\vec{u}$  is null everywhere. If we decrease particle density, the pattern obtained is basically the same, as we can verify through Figure 7.

The configuration of pictured on Figure 2 can be generalized by an initial density with a disconnected zero set. Figure 10-a pictures such example. We get an interesting pattern formation presented on Figure 10-b. These patterns evolve to the "S" formations pictured on Figure 11.

Besides, we can take advantage of the simplicity of the model for changing boundary. For a LGCA, there is no need to re-build the lattice. It is just a matter of finding the boundary cells of the lattice and apply the proper collision rules for particles entering the corresponding sites. Next, we show the tests using a homogeneous particles distribution with velocity in the horizontal direction. It is interesting to observe the patterns at the right hand side of the Figure 9. Particles that collide with the domain boundary also will collide with the incident particles which increases the density nearby.

## 5. Conclusions

In this paper we propose the FHP model for fluid modeling in computer graphics applications. We discuss the theoretical elements of our proposal and discuss some experimental results. Further works are the incorporation of external forces and model two-phase systems for visual effects generation.

## References

- [1] In *SCA '04: Proceedings of the 2004 ACM SIGGRAPH/Eurographics symposium on Computer animation*, New York, NY, USA, 2004. ACM Press.
- [2] B. Chopard and M. Droz. *Cellular Automata Modeling of Physical Systems*. Cambridge University Press, 1998.
- [3] M. Desbrun and M. P. Cani. Smoothed particles: A new paradigm for animating highly deformable bodies. In *Proceedings of EG Workshop on Animation and Simulation*, pages 61–76. Springer-Verlag, 1996.
- [4] G. Doolen. *Lattice Gas Method for Partial Differential Equations*. Addison-Wesley, 1990.
- [5] N. Foster and D. Metaxas. Modeling the motion of a hot, turbulent gas. In *ACM SIGGRAPH*, pages 181–188. ACM Press, 1997.
- [6] U. Frisch, D. D'Humières, B. Hasslacher, P. Lallemand, Y. Pomeau, and J.-P. Rivet. Lattice gas hydrodynamics in two and three dimension. *Complex Systems*, pages 649–707, 1987.
- [7] U. Frisch, B. Hasslacher, and Y. Pomeau. Lattice-gas automata for the navier-stokes equation. *Phys. Rev.*, page 1505, 1986.
- [8] J. Harting, J. Chin, M. Venturoli, and P. V. Coveney. Large-scale lattice boltzmann simulations of complex fluids: advances through the advent of computational grids. <http://www.ica1.uni-stuttgart.de/~jens/pub/05/05-PhilTransReview.pdf>, 2005.
- [9] C. Hirsch. *Numerical Computation of Internal and External Flows: Fundamentals of Numerical Discretization*. John Wiley Sons, 1988.
- [10] T. Inamuro, T. Ogata, and F. Ogino. Numerical simulation of bubble flows by the lattice boltzmann method. *FUTURE GENERATION COMPUTER SYSTEMS*, 20(6):959–964, 2004.
- [11] J. Mark, G. Harris, and C. T. S. A. L. Physically-based visual simulation on graphics hardware. *Graphics Hardware*, pages 1–10, 2002.
- [12] J. Morris, P. Fox, and Y. Zhu. Modeling low reynolds number incompressible flows using sph. *JOURNAL OF COMPUTATIONAL PHYSICS*, 136:214–226, 1997.
- [13] M. Müller, D. Charypar, and M. Gross. Particle-based fluid simulation for interactive applications. In *Proceedings of ACM SIGGRAPH symposium on Computer animation*, 2003.
- [14] M. Müller, R. Keiser, A. Nealen, M. Pauly, M. Gross, and M. Alexa. Point based animation of elastic, plastic and melting objects. In *SCA '04: Proceedings of the 2004 ACM SIGGRAPH/Eurographics symposium on Computer animation*, pages 141–151, New York, NY, USA, 2004. ACM Press.
- [15] M. Müller, S. Schirm, and M. Teschner. Interactive blood simulation for virtual surgery based on smoothed particle hydrodynamics. *Technol. Health Care*, 12(1):25–31, 2004.
- [16] M. Müller, S. Schirm, M. Teschner, B. Heidelberger, and M. Gross. Interaction of fluids with deformable solids. In *SCA '04: Proceedings of the 2004 ACM SIGGRAPH/Eurographics symposium on Computer animation*, New York, NY, USA, 2004. ACM Press.
- [17] D. Nguyen, D. Enright, and R. Fedkiw. Simulation and animation of fire and other natural phenomena in the visual effects industry. *Western States Section, Combustion Institute, Fall Meeting, UCLA*, 2003.
- [18] J. Piasecki. *Echelles de temps multiples en théories cinétique. Cahiers de physique*. Press polytechniques et universitaire romandes, 1997.
- [19] S. Premoze, T. Tasdizen, J. Bigler, A. Lefohn, and R. Whitaker. Particle-based simulation of fluids. In *EUROGRAPHICS*, volume 22, 2003.
- [20] L. Rosemblum, R. Earnshaw, J. Encarnacao, H. Hagen, A. Kaufman, S. Klimenko, G. Nielson, F. Post, and D. Thalmann. *Scientific Visualization: Advances and Challenges*. Academic Press, 1994.
- [21] B. Schlatter. A pedagogical tool using smoothed particle hydrodynamics to model fluid flow past a system of cylinders. Master's thesis, 1989.
- [22] J. Stam. Stable fluids. In *Proceedings of the 26th annual conference on Computer graphics and interactive techniques*, pages 121–128. ACM Press/Addison-Wesley Publishing Co., 1999.
- [23] J. Stam. Real-time fluid dynamics for games. In *Proceedings of the Game Developer Conference*, 2003.
- [24] N. Thalmann and D. Thalmann, editors. *New Trends in Animation and Visualization*. John Wiley & Sons, 1991.
- [25] P. Witting. Computational fluid dynamics in a traditional animation environment. In *SIGGRAPH '99: Proceedings of the 26th annual conference on Computer graphics and interactive techniques*, pages 129–136. ACM Press/Addison-Wesley Publishing Co., 1999.
- [26] S. Wolfram. *Cellular automata and complexity*. Addison-Wesley, <http://www.stephenwolfram.com/publications/articles/ca/86-fluids/index.html>, 1996.

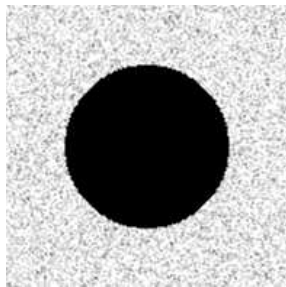


Figure 2: Initial configuration with 80000

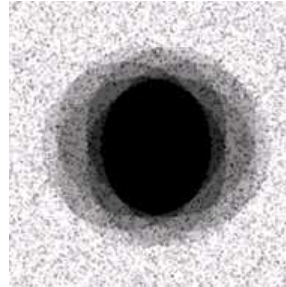


Figure 3: Evolution after 10 steps

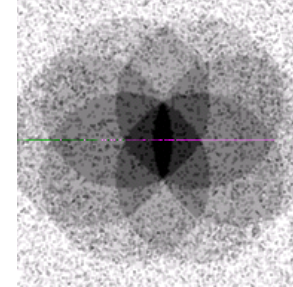


Figure 4: Evolution after 25 steps

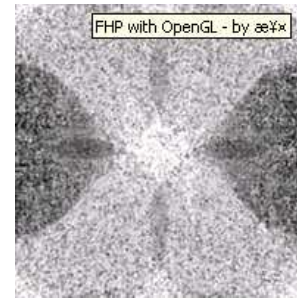


Figure 5: Evolution after 50 steps

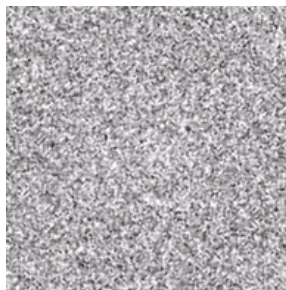


Figure 6: Evolution after 300 steps

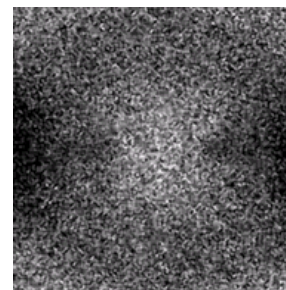


Figure 7: 40000 particles after 50 steps



Figure 8: Horizontal velocity pattern

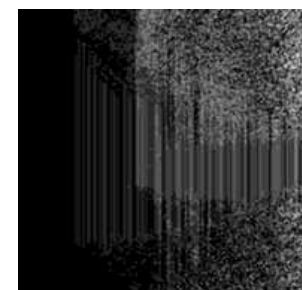
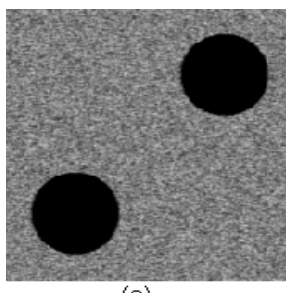
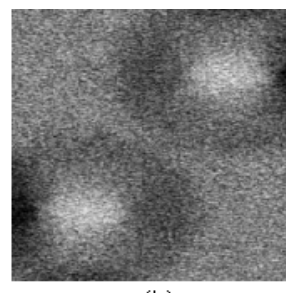


Figure 9: Evolution after 100 steps of Figure 7

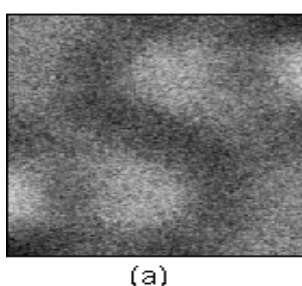


(a)

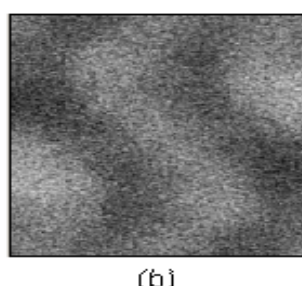


(b)

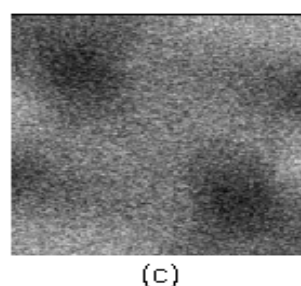
Figure 10: (a) Initial configuration. (b) Transient pattern formation.



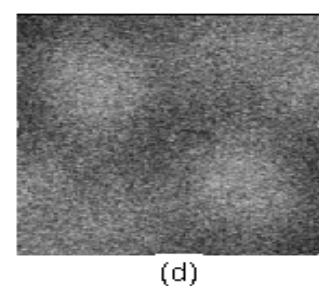
(a)



(b)



(c)



(d)

Figure 11: Evolution of the configuration pictured on Figure 9-a.